Comparative Analysis of the Circle Fitting Empirical Method and the International Telecommunication Union Parabola Fitting Method for Determination of the Radius of Curvature for Rounded Edge Diffraction Obstruction

Simeon Ozuomba
Department of
Electrical/Electronic and
Computer Engineering University
of Uyo
Akwa Ibom State Nigeria

Constant Kalu
Department of
Electrical/Electronic and
Computer Engineering University
of Uyo
Akwa Ibom State Nigeri.

Henry Johnson Enyenihi
Department of
Electrical/Electronic Engineering,
Akwa Ibom State University
Mkpat Enin,
Akwa Ibom State Nigeria

ABSTRACT
In this paper, comparative analysis of the circle fitting empirical method and the parabola fitting method for determination of the radius of curvature for rounded edge diffraction obstruction was presented. Sample elevation profile data for a 40 Km path with hilly obstruction was collected using web-based Geocontext elevation profile tool. The maximum elevation of 307.4569 m occurred at a distance of 35966.33 m the maximum elevation point from the transmitter. The two radius of curvature methods were applied to the elevation data. The exact radius of curvature based on the circle fitting empirical method is 38,375.22 m whereas the radius of curvature based on the International Telecommunication Union (ITU) parabola fitting method is 34, 029.98 m. Furthermore, while the radius by the empirical circle fitting method remained the same under different microwave frequencies, for the ITU parabola fitting method, there was over 89 % reduction in the radius of curvature from 60,369.69 m at 1 GHz L-band microwave frequency to 11,476.36 m at 12 GHz Ku-band microwave frequency. The essence of this study is to demonstrate the wide variation in the radius of curvature due to the frequency and also to advise that the ITU method may be used only when the ITU method of rounded edge diffraction loss is employed. The other rounded edge diffraction loss methods can use other approximation methods that compare favorably with the exact radius in all frequencies.

Keywords
Diffraction loss, rounded obstruction, parabola fitting method, radius of curvature, wireless communication.

1. INTRODUCTION
Nowadays , there is wide adoption of wireless communication across the globe [1,2,3,4]. As the adoption of wireless communication increases, experts are facing running challenges in providing adequate quality of service to the teeming population of wireless communication network users. One of the challenges in wireless communication is the diffraction loss due to obstructions in the path of the wireless signal [5,6,7,8,9,10]. Obstructions like mountains and trees are in some cases modeled as knife-edge obstructions [11,12,13,14,15,16,17,18]. However, further studies revealed that single knife-edge model of such obstruction usually underestimate the actual diffraction loss posed by obstructions like hills. In respect of this finding, for hilly obstructions , rounded edge obstruction model is usually used instead of the knife-edge model [19,20,21].

Generally, in the rounded edge obstruction model, a curve is fitted to the vicinity of the hill apex. The radius of curvature of such curve along with angles made by tangent lines to the curve is then used in the computation of the rounded edge diffraction loss. One of the popular methods of generating the curve is by fitting a circle to the vicinity of the hill apex. However, the International Telecommunication Union (ITU) developed a parabolic curve fitting reproach for the rounded edge diffraction loss computation [22]. Remarkably, based on the underlying formula and constraint presented by ITU, the radius of the parabolic curvature is affected by the frequency of the signal. In this paper, comparative study of the ITU parabola fitting method and the circle fitting method for determination of the radius of curvature of rounded edge obstruction is presented. Specifically, for the circle fitting method, the exact radius of curvature is obtained using empirical measurements conducted on the path elevation profile plot of the hilly obstruction along the signal path. The study is meant to show the disparity in the values of the radius of curvature obtained using the two methods and how the values vary with respect to the frequency.

2. THE RADIUS OF CURVATURE BY THE ITU PARABOLA FITTING METHOD
Unlike the other approximate method that tends to use radius of circle to determine the radius of curvature for rounded edge diffraction loss computation, the International Telecommunication Union (ITU) uses a parabolic fitting approach whereby a parabola is fitted to the vicinity of the obstruction apex. The ITU approach requires that the maximum vertical distance from the apex of the obstruction should be about the same as the radius of the first Fresnel zone computed at the point where the obstruction apex is located. The parabola along with the parameters used for the ITU parabola fitting method is shown in Figure 1 '
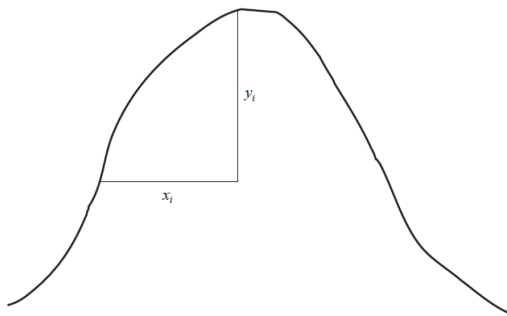
Figure 1 The parabola along with the parameters used for the ITU parabola fitting method

First, the radius of the first Fresnel zone at the apex of the obstruction is computed as follows [23];

$$R_{f1} = 17.32 \left(\sqrt{\frac{(d_{ta})(d_{ra})}{f(d_t a + d_{ra})}} \right) \tag{1}$$

Where f is frequency in GHz and d_{ta} in Km is the distance of the obstruction apex from the transmitter while d_{ra} in Km is the distance of the obstruction apex from the receiver.

Then, based on Figure 1 and the ITU parabolic fitting approach , if E_a is the elevation of the obstruction apex, then all elevation data points with elevation E_i such that $E_a - E_i \leq R_{f1}$ are used in the computation of the parabola parameter. Now, if the coordinates of the obstruction apex is given as d_a, E_a and there are Na elevation data points that satisfy the condition that $E_a - E_i \leq R_{f1}$, then the radius of curvature, r_i of the parabola at elevation point i with distance and elevation coordinates given as d_i, E_i is computed as follows [22] ;

$$x_i = d_a - d_i \qquad \text{for i =1,2,3,…,Na} \tag{2}$$

$$y_i = E_a - E_i \qquad \text{for i =1,2,3,…,Na} \tag{3}$$

$$r_i = \frac{x_i{}^2}{2(Y_i)} \qquad \text{for i =1,2,3,…,Na} \tag{4}$$

Eventually, the median radius of curvature of the obstacle is given by [22]:

$$R = \frac{1}{Na} \left[\sum_{i=1}^{i=n} \left(\frac{x_i{}^2}{2Y_i} \right) \right] \tag{5}$$

3. THE EMPIRICAL METHOD FOR COMPUTING THE EXACT RADIUS OF CURVATURE FOR ROUNDED EDGE DIFFRACTION OBSTRUCTION

Unlike the ITU method that fits in a parabola to the vicinity of the apex of the hilly obstruction, the exact method fits in a circle, as shown in Figure 2. So, the focus of the exact method is to determine the radius of the circle.
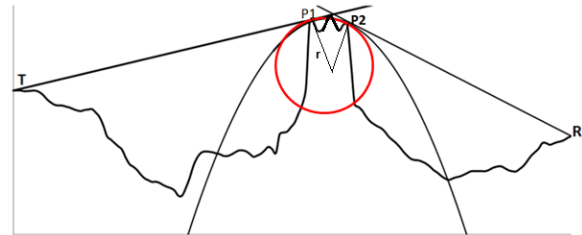

Figure 2 The path profile of the Hilly obstruction along with the sketch of the circle to be fitted by the exact method and the parabola to be fitted by the ITU method

In order to determine the radius of the circle, first, a tangent line TP_1 is drawn from the transmitter, T to the path profile, which in this case is tangential at point P_1. A tangent line RP_2 is drawn from the receiver, R to the path profile, which in this case is tangential at point P_2. Line TP_1 and line RP_2 are extended to intersect at V , as shown in Figure 3. A line perpendicular to line TP_1 is drawn at point P_1. Another line perpendicular to line RP_2 is drawn at point P3. The intersection of the two perpendicular line at point C gives the center of the circle. The line CP1 is the radius of the circle and it can be measured using a ruler. A protractor can be used to measure the relevant angles namely, β1, β2 and α . Also, the clearance height, h can also be measured using a ruler. Other lines that their lengths are needed to be measured are line TP1, RP1, the occultation distance P1P2 or line FG which is the horizontal distance between point P1 and point P2; line BR which is the path length or the distance between the transmitter and the receiver. Line BT which is the difference in the elevation between the transmitter and the receiver.
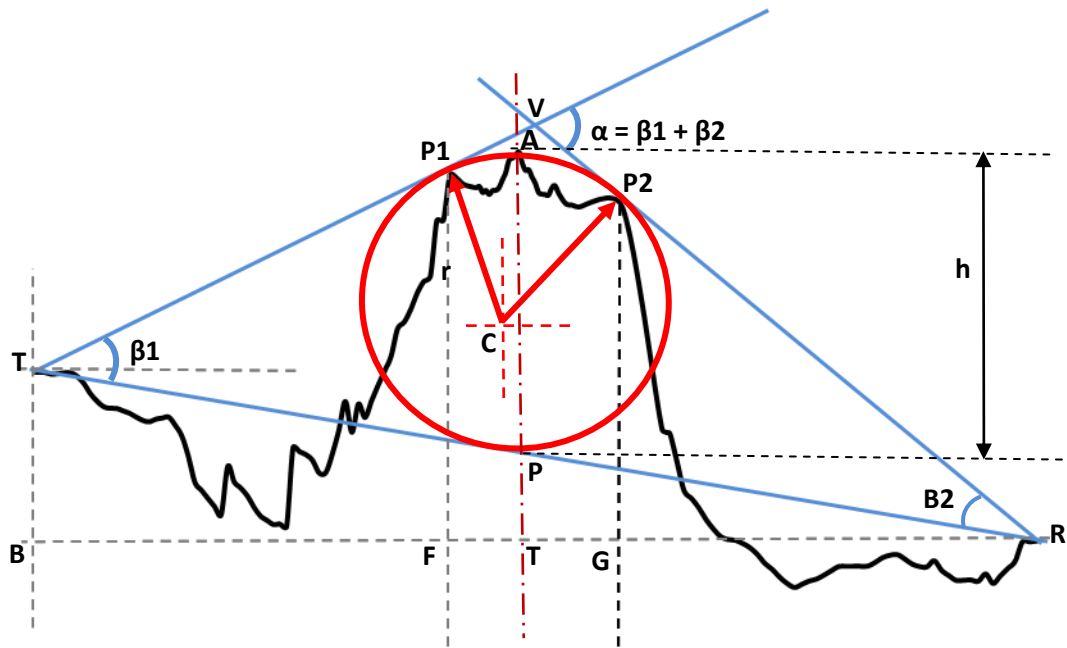
Figure 3 The detail path profile and parameters used in the exact method

4. RESULTS AND DISCUSSIONS

Sample elevation profile data was obtained using the Geocontext elevation profile web application. The elevation profile data obtained for a path with the hilly obstruction is given in Table 1 and Figure 4 .

In Table 2, the maximum elevation is 307.4569, the distance of the maximum elevation point from the transmitter , $d_{ta} = 35966.33$ m , the distance of the maximum elevation point from the receiver , $d_{ra} = 4033.66847$ m , the frequency is 4 GHz, so the radius of the first Fresnel zone at the maximum elevation point is 16.49248 m. As such in

Table 2 , all the that are used to determine the parabola curvature must be such that their y_i are less than 16.49248 . That is what is shown in Table 2 , all the $y_i \leq 16.49248$. In all, there are 44 elevation points that satisfied the condition and the sum of $\left(\frac{x_i^2}{2(y_i)}\right)$ obtained from that 44 points is 1497319.3 m, so the parabola curvature radius is 1497319.3/44 = 34, 029.98 m. However, the exact radius obtained from the empirical measurement based on the elevation profile data is 38,375.22 m.

Table 1 The elevation profile data of the path with the hilly obstruction

Data points 1 to 30		Data points 31 to 60		Data points 61 to 90		Data points 91 to 120		Data points 121 to 150	
Distance (m)	Elevation (m)	Distance (m)	Elevation (m)	Distance (m)	Elevation (m)	Distance (m)	Elevation (m)	Distance (m)	Elevation (m)
0.0	233.2	18502.1	255.1	35282.2	299.0	36565.0	297.4	38114.7	250.9
616.7	232.7	19118.8	255.4	35324.9	298.0	36607.7	297.8	38179.8	248.9
1233.5	232.5	19735.5	255.6	35367.7	297.7	36650.5	298.5	38244.8	245.8
1850.2	232.0	20352.3	255.9	35410.5	297.6	36693.2	295.5	38309.8	242.1
2466.9	231.4	20969.0	256.4	35453.2	298.4	36736.0	295.0	38374.8	229.9
3083.7	231.4	21585.7	257.0	35496.0	299.3	36778.8	293.9	38439.8	227.4
3700.4	231.4	22202.5	257.7	35538.7	300.2	36821.5	292.6	38504.8	225.9
4317.1	232.7	22819.2	258.7	35581.5	301.0	36864.3	291.2	38569.8	226.1
4933.9	233.5	23435.9	259.8	35624.3	301.7	36907.0	290.1	38634.8	225.0

|									
5550.6	234.3	24052.7	261.4	35667.0	302.3	36949.8	289.3	38699.8	224.5
6167.4	235.1	24669.4	262.6	35709.8	302.6	36992.6	288.3	38764.8	215.3
6784.1	235.7	25286.1	262.8	35752.5	301.6	37035.3	287.3	38829.8	210.7
7400.8	236.3	25902.9	263.3	35795.3	301.9	37078.1	289.4	38894.9	209.6
8017.6	236.9	26519.6	264.2	35838.1	304.7	37120.8	288.0	38959.9	208.3
8634.3	237.7	27136.3	265.6	35880.8	304.7	37163.6	289.9	39024.9	206.8
9251.0	238.3	27753.1	267.2	35923.6	306.5	37206.4	288.8	39089.9	190.4
9867.8	238.8	28369.8	268.8	35966.3	307.5	37249.1	285.8	39154.9	186.6
10484.5	239.8	28986.5	270.4	36009.1	306.3	37291.9	285.6	39219.9	183.3
11101.2	240.9	29603.3	272.3	36051.9	305.1	37334.6	285.7	39284.9	184.0
11718.0	242.4	30220.0	274.7	36094.6	304.2	37399.7	282.2	39349.9	181.1
12334.7	243.8	30836.8	277.8	36137.4	303.5	37464.7	281.7	39414.9	178.4
12951.4	245.4	31453.5	280.9	36180.1	303.0	37529.7	267.3	39479.9	180.4
13568.2	246.7	32070.2	290.6	36222.9	302.5	37594.7	264.7	39544.9	180.4
14184.9	247.5	32687.0	293.0	36265.7	302.1	37659.7	262.6	39609.9	181.7
14801.6	248.3	33303.7	294.9	36308.4	301.6	37724.7	260.4	39675.0	182.5
15418.4	249.1	33920.4	296.1	36351.2	301.1	37789.7	258.1	39740.0	183.2
16035.1	250.3	34537.2	297.3	36393.9	297.0	37854.7	256.0	39805.0	186.9
16651.8	251.7	35153.9	298.4	36436.7	296.9	37919.7	254.5	39870.0	185.6
17268.6	253.3	35196.7	299.4	36479.4	296.8	37984.7	253.1	39935.0	186.4
17885.3	254.6	35239.4	299.4	36522.2	297.1	38049.7	251.8	40000.0	187.9
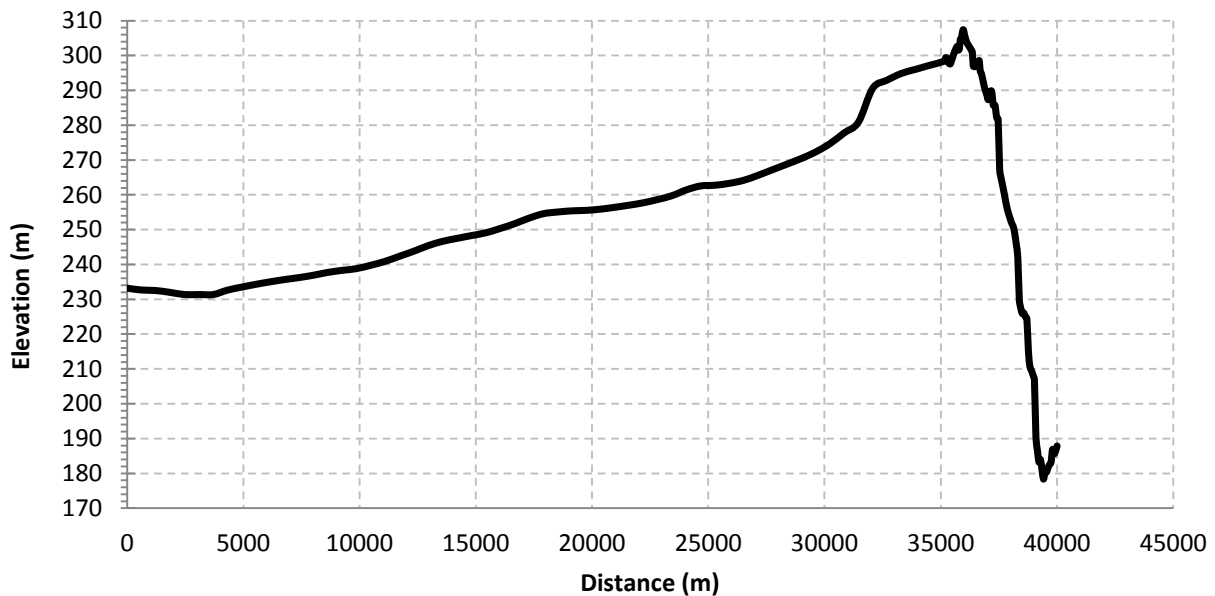
Figure 4 The elevation profile data plot for the path with the hilly obstruction

Table 2 The Portion of the elevation data points that were used in the ITU parabola fitting approach at the Frequency of 4 GHz and path length of 40 Km

S/N i	Elevation Data Point Number	x_i	y_i	$\frac{x_i^2}{2(y_i)}$	S/N	Elevation Data Point Number	x_i	y_i	$\frac{x_i^2}{2(y_i)}$
1	53	3,279	14.5	370,773	23	75	43	0.9	970
2	54	2,663	12.6	281,975	24	76	43	1.2	763
3	55	2,046	11.4	183,809	25	77	86	2.3	1,563
4	56	1,429	10.2	100,076	26	78	128	3.3	2,522
5	57	812	9.0	36,549	27	79	171	4.0	3,680
6	58	770	8.1	36,567	28	80	214	4.4	5,184
7	59	727	8.0	32,852	29	81	257	4.9	6,700
8	60	684	8.5	27,625	30	82	299.3	5.3	8420.2
9	61	641	9.4	21,856	31	83	342.1	5.9	9906.5
10	62	599	9.8	18,338	32	84	384.8	6.3	11679.7
11	63	556	9.8	15,717	33	85	427.6	10.5	8714.4
12	64	513	9.0	14,605	34	86	470.4	10.6	10437.2
13	65	470	8.2	13,497	35	87	513.1	10.6	12393.5
14	66	428	7.3	12,537	36	88	555.9	10.4	14846.1
15	67	385	6.5	11,391	37	89	598.6	10.0	17838.0
16	68	342	5.8	10,089	38	90	641.4	9.6	21396.1
17	69	299	5.2	8,612	39	91	684.2	9.0	26148.0
18	70	257	4.8	6,790	40	92	726.9	11.9	22179.1
19	71	214	5.9	3,879	41	93	769.7	12.5	23784.4
20	72	171	5.6	2,617	42	94	812.4	13.6	24280.3
21	73	128	2.8	2,991	43	95	855.2	14.9	24560.2
22	74	86	2.7	1,344	44	96	898.0	16.2	24863.7
								SUM	1497319.3

For the given elevation profile data, the radius of the rounded edge fitted in the vicinity of the hilly obstruction apex was determined for a number of frequencies and the results are given in Table 3. The results show that the radius of curvature by the ITU method is significantly affected by the frequency. There was over 89 % reduction in the radius of curvature from 60,369.69 m at   1 GHz L-band microwave frequency to 11,476.36 m at 12 GHz Ku-band microwave frequency. On the other hand, the exact radius by circle fitting empirical method did not change with the frequency. The essence of this study is to demonstrate this wide variation in the radius of curvature due to the frequency and also to advise that the ITU method may be used only when the ITU method of rounded edge diffraction loss is employed. The other rounded edge diffraction loss methods can use other approximation methods that compare favorably with the exact radius in all the frequencies.

Table 3 The radius of the rounded edge fitted in the vicinity of the hilly obstruction apex for different frequencies

Microwave Frequency Band	Frequency (GHz)	Radius of the first Fresnel zone (m)	Number of elevation data points used in the ITU Parabola Fitting Method	Radius of curvature by ITU Parabola Fitting Method (m)	Radius of curvature by Empirical Circle Fitting Exact Radius Method (m)
L-Band	1	32.98496781	62	60,369.69	38,375.22
L-Band	2	23.32389	57	40,848.07	38,375.22
C-Band	4	16.49248	44	34,029.98	38,375.22

C-Band	6	13.46606	41	25,679.07	38,375.22
Ku-Band	12	9.52194	28	11,476.36	38,375.22

5. CONCLUSION

The radius of curvature for rounded edge diffraction loss computation is determined using two different methods are presented. The methods are , one , the circle fitting empirical method which gives the exact radius for the circle and two, the International Telecommunication Union (ITU) parabola fitting method which fits a parabola to the vicinity of the obstruction apex. Requisite analytical expressions for the two methods are presented. A sample elevation profile data for the path with the hilly obstruction was collected and used to examine the effect of the frequency on the radius of curvature obtained using each of the two methods. The exact radius of curvature based on the circle fitting empirical method maintained the same value of the radius of curvature under different microwave frequencies. However, the ITU parabola fitting method gave over 89 % reduction in the radius of curvature when the frequency was varied from 1 GHz L-band microwave frequency to 12 GHz Ku-band microwave frequency. The study clearly demonstrated that for the ITU parabola fitting method there is wide variation in the radius of curvature due to the frequency.

6. REFERENCES

[1] Zheng, L., Lu, N., & Cai, L. (2013). Reliable Wireless Communication Networks for Demand Response Control. *IEEE Trans. Smart Grid*, *4*(1), 133-140.

[2] Akyol, B. A., Kirkham, H., Clements, S. L., & Hadley, M. D. (2010). *A survey of wireless communications for the electric power system* (No. PNNL-19084). Pacific Northwest National Lab.(PNNL), Richland, WA (United States).

[3] Omogbadegun, Z. O., & Ayo, C. K. (2007). Impact of mobile and wireless technology on healthcare delivery services. *3GSM & Mobile Computing: An Emerging Growth Engine for National Development*, 164-171.

[4] Valenzuela, R. A., & Kocan, K. F. (2005). Future wireless communications. *Bell Labs Technical Journal*, *10*(2), 1-3.

[5] *Niu*, Y., Li, Y., Jin, D., Su, L., & Vasilakos, A. V. (2015). A survey of millimeter wave communications (mmWave) for 5G: opportunities and challenges. *Wireless Networks*, *21*(8), 2657-2676.

[6] Al-Hourani, A., Kandeepan, S., & Jamalipour, A. (2014, December). Modeling air-to-ground path loss for low altitude platforms in urban environments. In *Global Communications Conference (GLOBECOM), 2014 IEEE* (pp. 2898-2904). IEEE.

[7] *Geng*, Y., He, J., & Pahlavan, K. (2013). Modeling the effect of human body on TOA based indoor human tracking. *International Journal of Wireless Information Networks*, *20*(4), 306-317.

[8] Savazzi, S., Guardiano, S., & Spagnolini, U. (2013). Wireless sensor network modeling and deployment challenges in oil and gas refinery plants. *International journal of distributed sensor networks*, *9*(3), 383168.

[9] Garg, V. (2010). *Wireless communications & networking*. Elsevier.

[10] Goldsmith, A. (2005). *Wireless communications*. Cambridge university press.

[11] Kasampalis, S. (2018). *Modelling and coverage improvement of DVB-T networks* (Doctoral dissertation, Brunel University London).

[12] Abdulrasool, A. S., Aziz, J. S., & Abou-Loukh, S. J. (2017). Calculation Algorithm for Diffraction Losses of Multiple Obstacles Based on Epstein–Peterson Approach. *International Journal of Antennas and Propagation*, *2017*.

[13]

[14] Zang, J., & Wang, X. (2017). Measurements and Modeling of Path Loss over Irregular Terrain for Near-Ground and Short-Range Communications. *Progress In Electromagnetics Research*, *57*, 55-62.

[15] Cid, E. L. (2017). *Lms and h-satcom channels characterization at x and ku bands* (Doctoral dissertation, Universidade de Vigo).

[16] Filiposka, S., & Trajanov, D. (2011). Terrain-aware three-dimensional radio-propagation model extension for NS-2. *Simulation*, *87*(1-2), 7-23.

[17] Kumar, K. A. M. (2011). Significance of Empirical and Physical Propagation Models to Calculate the Excess Path Loss. *Journal of Engineering Research and Studies E-ISSN*, *976*, 7916.

[18] Milanović, J., Rimac-Drlje, S., & Majerski, I. (2010). Radio wave propagation mechanisms and empirical models for fixed wireless access systems. *Tehnički vjesnik*, *17*(1), 43-53.

[19] Uko, M. C., Udoka, U. E., & Nkwocha, C. P. (2017). Parametric Analysis of Isolated Doubled Edged Hill Diffraction Loss Based on Rounded Edge Diffraction Loss Method and Different Radius of Curvature Methods. *Mathematical and Software Engineering*, *3*(2), 217-225.

[20] Poisel, R. (2011). *Modern Communications Jamming: Principles and Techniques*. Artech House.

[21] Vélez, M. M., Angueira, P., De la Vega, D., Arrinda, A., Ordiales, J. L., & Vicente, A. S. (2000). Ground Profile Analysis Algorithm To Improve Multiple Diffraction Loss Estimation. In *Proceedings Of The International Symposium On Antennas And Propagation Japan* (Vol. 3, pp. 1347-1350).

[22] Series, P. (2018). Propagation by diffraction. Recommendation ITU-R P.526-14. Available at https://www.itu.int/dms_pubrec/itu-r/rec/p/R-REC-P.526-14-201801-I!!PDF-E.pdf. Accessed on November 12 2018.

[23] Akkasli, C. (2009). Methods for Path loss Prediction. Master thesis at School of Mathematics and Systems Engineering